THE ASTROPHYSICAL JOURNAL, 236: 388–405, 1980 March 1

THE NEBULOSITY ASSOCIATED WITH 3C 120

J. A. BALDWIN[1] AND R. F. CARSWELL
Institute of Astronomy, Cambridge, England
E. J. WAMPLER
Lick Observatory, Board of Studies in Astronomy and Astrophysics, University of California, Santa Cruz
HARDING E. SMITH[2] AND E. M. BURBIDGE[2]
Department of Physics, University of California, San Diego
AND
A. BOKSENBERG
Department of Physics and Astronomy, University College London
Received 1979 May 15; accepted 1979 September 13

ABSTRACT

We have made spectrophotometric observations of the nebulosity surrounding the Seyfert (or N) galaxy 3C 120, as well as of the nucleus. Our observations of the nebulosity reveal an extensive network of H II regions characterized by a high ionization level, which we argue is due to photoionizations by the nucleus. The O/H and N/O abundance ratios in this gas, at least as far out as 8 kpc from the nucleus, must be within a factor of 20 of the solar values. The velocity field of this gas is very chaotic, but the systematic gas velocities, relative to the nucleus, are mostly positive to one side of an axis passing through the nucleus at P.A. 72° and mostly negative on the other side. The position angle of this axis is consistent with the direction (P.A. 65°) along which the compact radio source in the nucleus is expanding, but it is about 45° away from the major or minor axes of the fainter elliptical structure visible on previously published broad-band direct plates. The spectrum of the nebulosity also has absorption lines which indicate an underlying galaxy containing a fairly normal stellar population and having essentially the same redshift as the emission lines.

Subject headings: galaxies: individual — galaxies: internal motions — galaxies: Seyfert — nebulae: abundances

I. INTRODUCTION

The extended optical object associated with 3C 120 has a starlike nucleus which varies between about 14 and 16 mag, and which has a strong emission-line spectrum with a redshift $z = 0.033$, (Burbidge 1967). The continuum radiation appears to be a nonthermal power law with an absolute magnitude $M_v \sim -21$. This places 3C 120 among the more luminous N galaxies or Seyfert galaxies (cf. Weedman 1976). Associated with this nucleus are strong X-ray and infrared sources (Schnopper *et al.* 1977; Rieke and Low 1972) and a powerful, compact (~ 1 pc) radio source, which has been reported to be expanding with apparently faster-than-light velocities (Cohen *et al.* 1977). In these respects 3C 120 presents physical problems which approach the same order of magnitude as those encountered for objects classified as QSOs.

The optical spectrum of the nucleus has been the subject of a number of studies (Wampler 1968; Shields, Oke, and Sargent 1972; Shields 1974; Phillips and Osterbrock 1975). The continuum energy distribution has been fitted with power-law spectra of the form $f_\nu \propto \nu^{-\alpha}$, with different observers finding values of α ranging from 0 to 1.8. The X-ray point would fit onto an extrapolation of an optical power-law spectrum with $\alpha \sim 1$, but the results from monitoring the nucleus with *UBV* photometry suggest that there may be two or more components varying in their relative intensities (Wlérick, Westerlund, and Garnier 1979). The emission-line spectrum has broad permitted lines with narrow forbidden lines and is typical of type 1 Seyferts and low-redshift quasars, with the exception that it has unusually strong helium lines (Phillips and Osterbrock 1975).

Surrounding this nucleus is a nebulosity of approximately 1′ diameter. This has usually been interpreted as a galaxy, on purely morphological grounds. Walker, Pike, and McGee (1974) showed that the isophotes have generally elliptical contours and therefore suggested that 3C 120 is a giant elliptical galaxy. However, a deep plate by Arp (1975) taken in good seeing shows that much of the light in the outer parts of the nebulosity comes from a series of knots arranged in roughly circular patterns, which Arp

[1] Also at Lick Observatory and Cerro Tololo Inter-American Observatory during parts of this investigation.

[2] Visiting Astronomer, Kitt Peak National Observatory, which is operated by the Association of Universities for Research in Astronomy, Inc., under contract with the National Science Foundation.

interpreted as spiral structure. Other studies of the isophotes of 3C 120 (Lelièvre 1976; Wlérick *et al.*) have confirmed the presence of an underlying, roughly elliptical structure extending some 25″ from the nucleus. The surface brightness falls off approximately as $r^{-1/4}$, but no firm morphological classification has been possible. The extent of the nebulosity, to a surface brightness $V = 25$ mag arcsec^{-2}, is 39″ × 65″ (31 × 52 kpc for $H_0 = 60$ km s^{-1} Mpc^{-1}). Arp (see Shields, Oke, and Sargent 1972) and Balick and Heckman (1979) have observed forbidden emission lines extending as far as 12″ out into the nebulosity. None of these previous studies have provided direct spectroscopic evidence for the presence of stars in 3C 120.

We consider 3C 120 to be one of the best examples of a luminous quasar-like object which is close enough to be studied with reasonable spatial resolution. We have therefore made a comprehensive spectroscopic study of 3C 120 aimed at understanding the nature of the nebulosity, especially the possible presence of a stellar population, and also aimed at studying the relationship of the nebulosity to the nonthermal continuum source.

Our observing program proceeded in two phases, which we describe separately below. First, a series of moderate-resolution (~7 Å) spectrophotometric scans were obtained of selected spots in the nebulosity. The nebulosity was then mapped at 1 Å resolution using the strongest emission line found in the lower-resolution scans.

II. LOW-RESOLUTION SPECTROPHOTOMETRY

a) Observations

We made spectrophotometric observations at about 7 Å resolution at 14 points across the surface of 3C 120, concentrating particularly on a 2″ × 8″ patch centered 10″ east of the nucleus. We also observed the nucleus, several prominent knots in the outer parts, and a few other points. Figure 1 shows the areas observed, and details are given in Table 1. These observations were made in the period 1973–1977, using Image Dissector Scanners (IDS) (Miller, Robinson, and Wampler 1975) on the 3 m Shane telescope of Lick Observatory, the 3.9 m Anglo-Australian telescope, and the 4 m Mayall telescope at Kitt Peak National Observatory.

TABLE 1

LOW-DISPERSION SPECTRA

Position	Date (U.T.)	Telescope	Aperture (arc-sec)	Wavelength Range (Å)
Nucleus	28 Oct. 73	Lick	2 x 2	3100-5450
"	15 Feb. 74	Lick	2 x 2	4580-7130
"	21 Feb. 74	Lick	2 x 4	4570-7130
"	17 Nov. 74	Lick	2 x 2	3450-5800
"	19 Nov. 74	Lick	2 x 4	3100-6500
"	16 Dec. 74	Lick	2 x 4	3320-5550
"	4 Oct. 75	AAT	2 x 2	4400-6320
"	7 Dec. 75	Lick	6 x 6	3900-5900
"	7 Dec. 75	KPNO	2 x 2	3230-6650
"	10 Oct. 77	Lick	6 x 6	3100-5300
Region 1	10 Oct. 77	Lick	2 x 8	3100-5300
"	11 Oct. 77	Lick	2 x 8	3380-5600
Region 2	15 Feb. 74	Lick	2 x 8	4460-6380
"	19 Nov. 74	Lick	2 x 8	3100-6500
"	16 Dec. 74	Lick	2 x 8	3320-5550
"	6 Dec. 75	KPNO	2 x 2	3230-6650
"	7 Dec. 75	KPNO	2 x 2	3230-6650
"	7 Dec. 75	Lick	2 x 8	3900-5900
"	7 Dec. 75	AAT	2 x 2	3660-6050
Region 3	4 Oct. 75	AAT	2 x 2	4400-6320
Region 4	4 Oct. 75	AAT	2 x 2	4400-6320
Region 5	7 Dec. 75	Lick	2 x 2	3900-5900
Region 6	5 Oct. 75	AAT	2 x 2	3100-6500
"	28 Jan. 76	Lick	2 x 2	3590-6000
"	29 Jan. 76	Lick	2 x 2	3590-6000
Region 7	28 Oct. 73	Lick	2 x 2	3100-5450
Region 8	3 Oct. 75	AAT	2 x 2	3660-6050
Region 9	5 Oct. 75	AAT	2 x 2	3100-6500
"	7 Dec. 75	Lick	2 x 2	3490-5900
Region 10	28 Jan. 76	Lick	2 x 2	3590-6000
"	28 Jan. 76	Lick	2 x 2	3590-6000
Region 11	3 Oct. 75	AAT	2 x 2	3660-6050
Region 12	3 Oct. 75	AAT	2 x 2	3660-6050
Region 13	3 Oct. 75	AAT	2 x 2	3660-6050

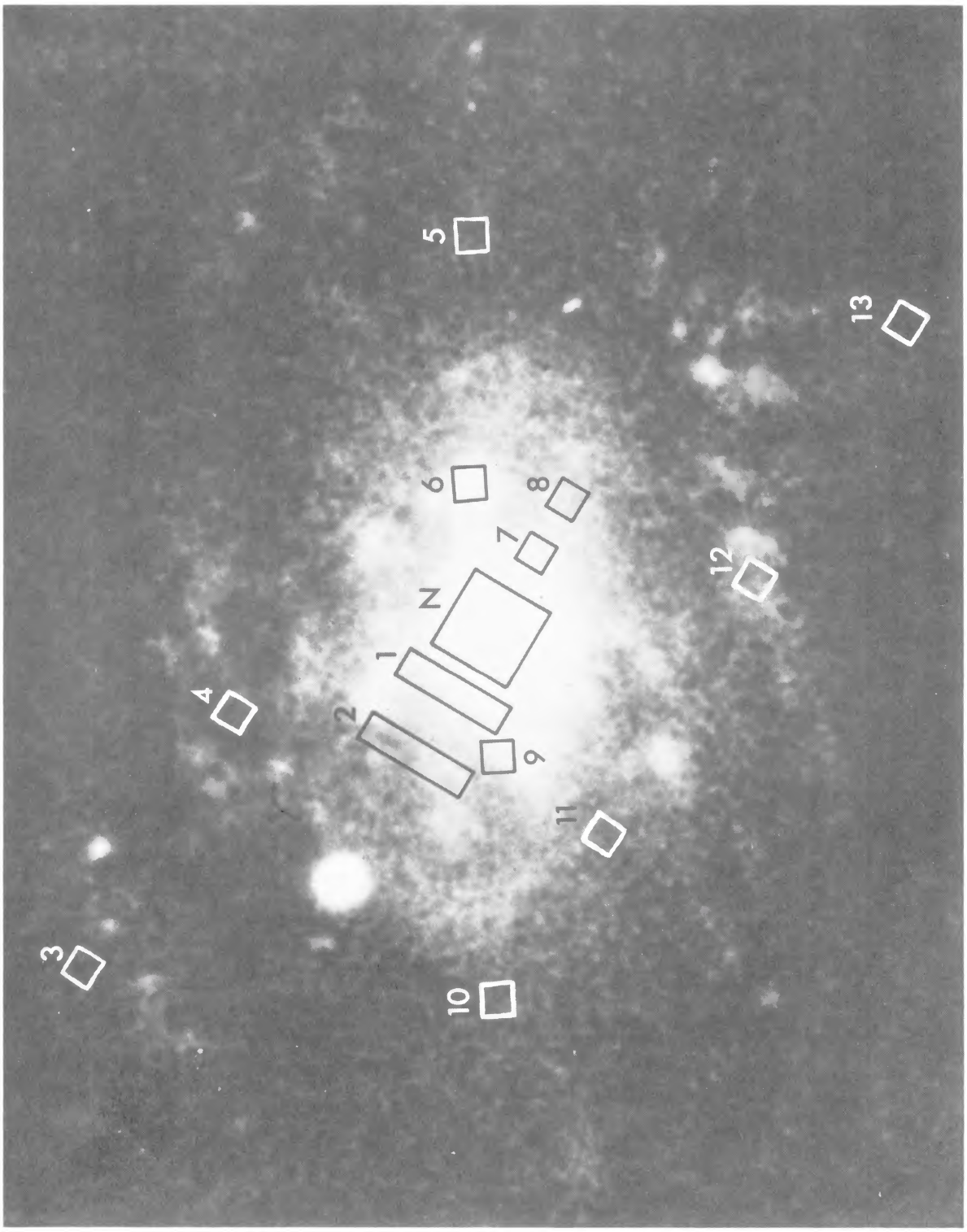

FIG. 1.—Direct plate of 3C 120 (from Arp 1975), with boxes showing regions observed with IDS. Position angle 27° is at the top of the figure; the bright star to the upper left is almost due east of the nucleus.

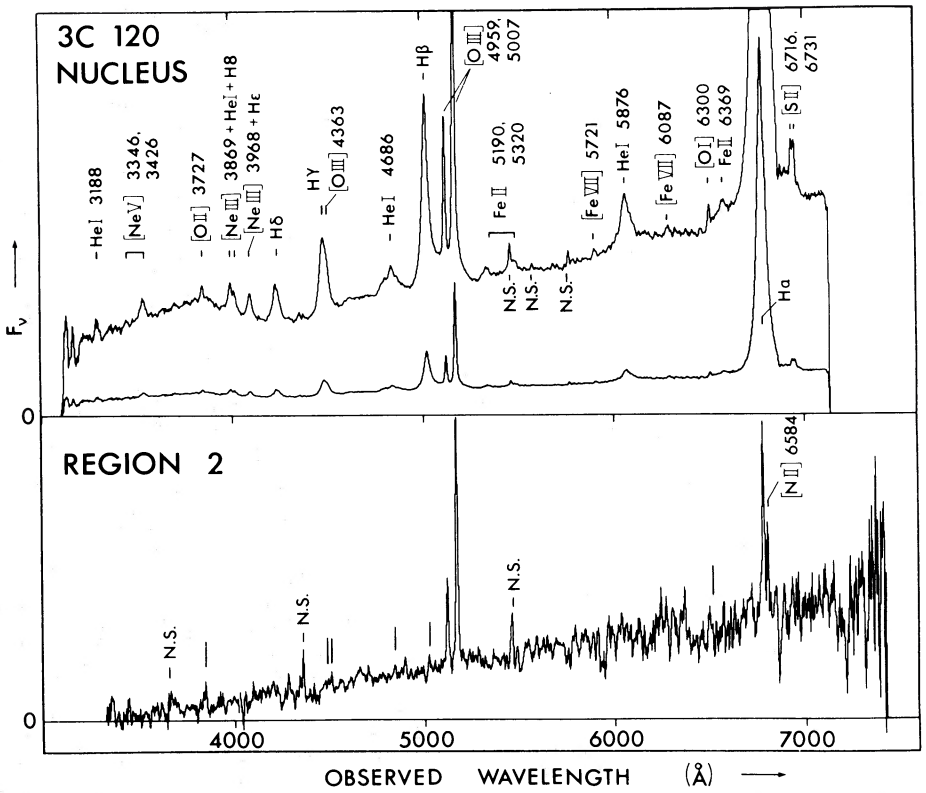

FIG. 2.—IDS scans of the nucleus and Region 2 of 3C 120. Emission lines discussed in the text or listed in Table 2 are marked. N.S. denotes position of night-sky lines.

The spectrum scans were reduced to absolute flux scales by means of spectrophotometric observations of secondary standard stars from the lists of Stone (1977) and Oke (1974). The scans of the nucleus of 3C 120 that were taken with large (6″ × 6″) entrance apertures give relative spectrophotometry which is accurate to a few percent, but only the night of 1973 Oct. 28 was of reasonable photometric quality. The scans of the nebulosity were always taken with a spectrograph slit width of ~2″, and with a slit length of either 2″ or 8″. Here again the majority of the nights were of inferior photometric quality, so that our measured fluxes are subject to wavelength-independent extinction.

b) The Nucleus

As there have been several detailed studies of the optical spectrum of the nucleus, we wish only to present our measurements of the line strengths and continuum energy distribution (Fig. 2 and Table 2) and to elaborate on a few pertinent points. We have relied on the line identifications made by Phillips and Osterbrock (1975) except as noted below.

The strengths of many of the lines are very difficult to measure because of the considerable amount of blending present. The problem was compounded by the very broad wings present in the instrumental profile of the IDS module used for most of the blue observations; for comparison, Figure 3 shows an uncalibrated scan of the Hβ region taken at 1 Å resolution with the IPCS (see § III). Following Phillips and Osterbrock, we have attempted to disentangle these blends in our IDS spectra by comparing the observed profiles with those of simulated blends synthesized from unblended profiles. We could not obtain unique solutions in the vicinities of Hγ and Hδ, which led us to obtain higher resolution observations of these spectral regions and of the Hβ emission line. These follow-up observations were made at 2.5 Å resolution, using the SIT-Vidicon system (Atwood *et al.* 1979) at the Cassegrain focus of the Cerro Tololo 4 m telescope on the nights of 1978 December 9 and 10.

Phillips and Osterbrock noted that the Hγ profile appears to be considerably broader than the Hα or Hβ profiles, and they fitted a synthesized blend of Hγ and [O III] λ4363 to this feature. The resulting [O III] λ4363/[O III] λ5007 intensity ratio is fairly large and implies a high temperature (2–3 × 10^4 K) and/or a high density ($N_e \geq 10^5$ cm^{-3}). The Hγ line also appears broader than Hβ in our IDS observations, but the higher resolution SIT data show the two profiles to be quite similar (although the SIT data are considerably noisier than those of the IDS observations). The SIT data show no sign of λ4363 emission, but there are clearly narrow spikes on top of both the Hγ and Hβ profiles (as can also be seen in Fig. 3),

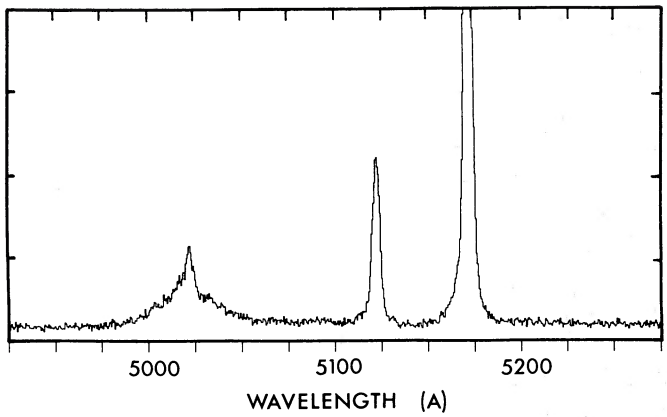

FIG. 3.—IPCS scan of the nucleus, showing the Hβ and [O III] λλ4959, 5007 emission lines

amounting to 5–10% of the total line strength. We suspect that the apparent difference between these profiles at lower resolution is due either to a difference in the relative strengths of the broad and narrow components of Hγ and Hβ, or to a slight difference in the instrumental resolution at the two lines. We therefore place an upper limit on the λ4363 strength that is about half that found by Phillips and Osterbrock.

Similarly, the measurement of the narrow [Ne III] λ3869 line on the wing of the Hδ + He I λ3889 blend is based on 2.5 Å resolution data. This region of the spectrum is very confused owing to the blending of the high Balmer lines, Hδ → H∞ and this has prevented us from making useful measurements of the other lines.

TABLE 2

EMISSION LINE INTENSITIES FOR THE NUCLEUS OF 3C 120

Line	I/I (Hβ)	Comments
He I 3188	0.12	
He II 3203	< 0.06	
[Ne V] 3346	0.03	Probably includes
[Ne V] 3426	0.15	Bowen O III lines
[O II] 3727	0.03	
[Ne III] 3869	0.10:	
He I + H8 3889	0.16:	
[Ne III] 3978 + Hε 3970	0.16	
[S II] 4071	< 0.02	
Hδ 4101	0.21	
Hγ 4340	0.55	Bad fit to Hβ profile
[O III] 4363	≤0.03	
N III 4641	0.08:	Blended
He II 4686	0.18	
Hβ 4861	1.00	
[O III] 4959	0.33	
[O III] 5007	1.00	
Fe II 5190	0.09	
Fe II 5320	0.10	
Fe VII 5721	0.01	
He I 5876	0.25	
[Fe VII] 6087	0.05	
[O I] 6300	0.02	
[O I] 6364 + Fe II, [Fe X] 6370	0.02	
Hα 6562	6.5	Blended
[N II] 6548	0.3:	
[S II] 6716	0.03	Blended
[S II] 6731	0.03	

The weak line blended with He II λ4686, which Phillips and Osterbrock suggested might be Fe II λ4629, gives a much better wavelength fit to N III multiplet 2 (λλ4634, 4641, 4642). This line is a by-product of the Bowen fluorescence mechanism (Bowen 1934), implying that the Bowen O III lines contribute appreciably to the λ3346 and λ3426 emission features.

The relative strengths of the N III lines and the line listed as λ3426 in Table 2 (which is an upper limit on the λ3444 strength) require a very high conversion efficiency, $R(\text{N III}) \gtrsim 1$, in the notation of Seaton (1960). Also, the Bowen mechanism implies the presence of strong He II λ304 emission, to excite the upper level of O III lines.

In addition to this indirect evidence for strong He II, an especially interesting feature of the spectrum of 3C 120 is the presence of exceptionally strong lines of He I λ5876 and He II λ4686. Phillips and Osterbrock (1975), MacAlpine (1976), and Feldman and MacAlpine (1978) have all found that the relative intensities of the He I triplet lines are far from the recombination values. It was suggested that the strength of λ5876 is increased as a result of some combination of collisional excitation and self-absorption effects in the triplet series. Our observations add λ3188 $4\,^3P$–$2\,^3S$ to the list of He I lines with measured intensities, with the surprising result that the λ3188/5876 intensity ratio is about the value expected from recombinations in the absence of any of the above effects or of any reddening. The helium line intensities are also not compatible with the moderately heavy reddening that would be implied by the steep Balmer decrement (Hα/Hβ ~ 6) in the simplest type of recombination model. The emission-line spectra of QSOs show similar inconsistencies with simple recombination plus reddening models (cf. Puetter *et al.* 1978; Puetter, Smith, and Willner 1979; Baldwin *et al.* 1978; Soifer *et al.* 1979, and references therein). Recent theoretical studies (Krolik and McKee 1979; Ferland and Netzer 1979; Canfield and Puetter 1980) suggest that radiation

transfer effects in very optically thick emission clouds may account for these apparent inconsistencies. The He II λ3202 line is not detected, but the λ3202/4686 intensity ratio must be less than 0.3, which is consistent with the value 0.27 calculated by Brocklehurst (1971) for case B recombinations.

The absolute calibration of our spectra of the nucleus is based on only one night (1973 Oct. 28), the other five scans having been obtained under nonphotometric conditions. The continuum of 3C 120 is known to be quite variable, but the strengths of the broad emission lines are thought to remain constant on time scales of several years (Shields, Oke, and Sargent 1972). We find the Hβ flux to be 2.1×10^{-13} ergs cm^{-2} s^{-1} Hz^{-1}. Although this is in reasonable agreement with the results of Adams and Weedman (1975), it is about half the values reported by Shields *et al.*, Wampler (1968), and Weedman (1976), so there exists the possibility of a wavelength-independent error in flux amounting to as much as a factor of 2. The continuum flux at 5000 Å is 2.1×10^{-26} ergs cm^{-2} s^{-1} Hz^{-1}, and the equivalent width of Hβ is 80 Å, both in the observed frame. The Balmer discontinuity is found to be 5.2×10^{-27} ergs cm^{-2} s^{-1} Hz^{-1}, which when compared to the Hβ flux gives a temperature $T_e \sim 6000$ K for case B, in good agreement with previous determinations. The continuum energy distribution on the long-wavelength side of the Balmer jump can be satisfactorily fitted with a power law $f_\nu \propto \nu^{-1.3}$ after correction for the hydrogen continuum emission.

c) *The Underlying Galaxy*

One of the objectives of this investigation was to determine whether the nebulosity surrounding the Seyfert nucleus of 3C 120 is, in fact, caused by stars in a galaxy. The area marked Region 1 in Figure 1 has a fairly high surface brightness but lies outside of the seeing disk of the nonthermal nucleus. Its spectrum (Fig. 4) shows definite evidence of a stellar population with a redshift of $z = 0.033$, in agreement with the emission-line redshift. Figure 4 also shows a comparison scan of an interarm region of the spiral galaxy M81, taken at a radial position which is approximately the same fraction of the Holmberg radius as that of Region 1 in 3C 120. The spectrum of Region 1 does not have a sufficiently high signal/noise ratio to allow us to distinguish between the late-type stellar population represented in M81 and that of a typical giant elliptical galaxy, but it is interesting to note that the widths of the absorption features suggest a smaller velocity dispersion in the disk of 3C 120 than in M81.

The spectrum of Region 2, the large patch 10″ east of the nucleus, is shown in Figure 2. Because of the low surface brightness, the signal/noise ratio is not high enough to allow an unambiguous identification of stellar absorption features, but the continuum is considerably stronger than would be expected from just the ionized gas that produces the emission lines, and the general shape of the continuum is very similar to that found for Region 1. The spectra of the other regions have much lower signal/noise ratios and provide no information about the stellar population.

d) *The Outlying Emission-Line Regions*

We detected narrow emission lines coming from most of the regions we observed. The absence of accompanying broad lines rules out the possibility that this is scattered light from the nucleus. The best spectrum is for Region 2 (see Fig. 2), in which the emission lines [O II] λ3727, [O III] λλ4959, 5007, [N II] λ6584, and Hα λ6562 can clearly be seen. There is also a probable line at the position of Hβ, and useful upper limits can be placed on the strengths of such lines as Hγ, [O III] λ4363, and [O I] λ6300. The relative intensities of these lines are listed in Table 3. We estimate the Hα/Hβ intensity ratio to be ~7, over twice the recombination value. This is consistent with reddening corresponding to $A_v \sim 2.5$ mag, or it might indicate that the strength of Hβ has been underestimated because part of the emission-line flux is being swallowed up by underlying absorption in the spectrum from the stellar population. Although there

TABLE 3

EMISSION LINE INTENSITIES FOR REGIONS 1 AND 2

LINE	I/I (5007)						
	Region 1	Region 2	NGC 1052[a] (shock heating)	Type 2 Seyfert[b]	3C 48[c]	3C 249.1[d]	4C 37.43[e]
[O II] 3727	0.20	0.17	3.6	0.27	0.44	0.40	0.15
Hγ 4340	< 0.08	< 0.04	0.21	0.04	...	...	0.02
[O III] 4363	< 0.08	< 0.04	0.08	0.02	...	...	0.02
He II 4686	< 0.08	< 0.04	...	0.03	...	...	...
Hβ 4861	0.08	≤0.06	0.44	0.09	...	0.16	...
[O III] 4959	0.29	0.34	0.33	0.33	0.24	0.34	0.25
[O III] 5007	1.00	1.00	1.00	1.00	1.00	1.00	1.00
He I 5876	...	< 0.12	...	0.01	...	...	...
[O I] 6300	...	< 0.17	0.65	0.05	...	...	...
Hα 6562	...	0.41	1.3	0.26	...	...	...
[N II] 6548+6584	...	0.22	1.8	0.28	...	...	...

REFERENCES.—[a] Fosbury *et al.* 1978. [b] Koski 1978. [c] Wampler *et al.* 1975. [d] Richstone and Oke 1977. [e] Stockton 1976.

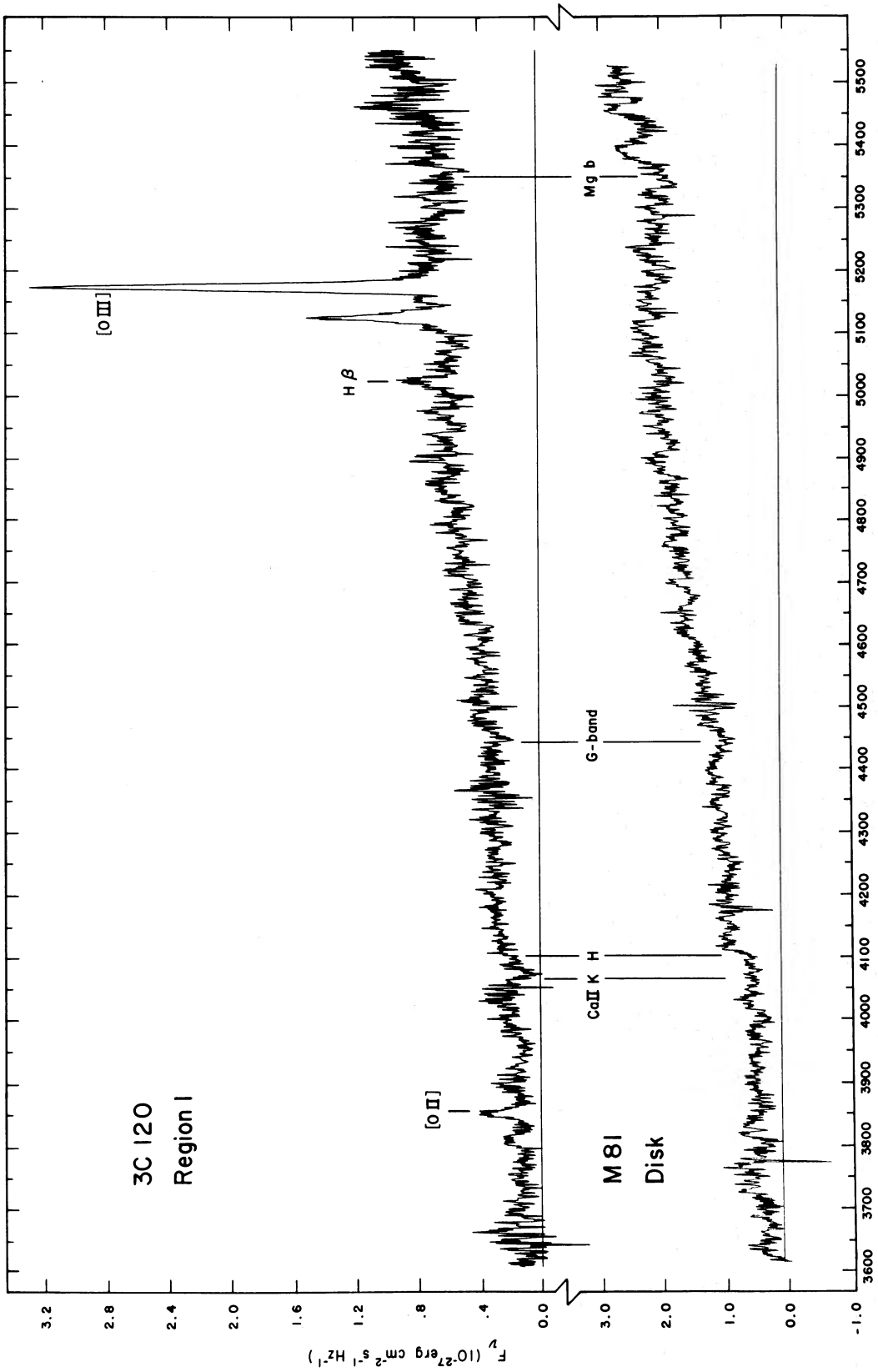

FIG. 4.—IDS scans of 3C 120 Region 1 and of a comparable interarm region in M81

is no strong absorption near the position of Hβ in the M81 spectrum, this is a common feature in the late-type spectra of the nuclei of galaxies.

We first consider the mechanism for ionizing this gas. It is unlikely that the gas is heated by shocks, because the [O I] λ6300 line is far weaker relative to [O III] λ5007 and [O II] λ3727 than is either predicted by shock models (Dopita 1977) or observed in radio galaxies in which the gas is thought to be heated by shocks, such as NGC 1052 (Fosbury *et al.* 1978). Line strengths for NGC 1052 are listed in Table 3 alongside those for 3C 120 to demonstrate this difference.

Photoionization thus remains as the most likely excitation mechanism. The observed [O III]/Hβ line ratio, even allowing for underlying absorption, is considerably larger than is observed in the spectra of normal H II regions in our Galaxy (Peimbert and Costero 1969) or at similar locations in other galaxies (Searle 1971; Smith 1975). In fact, the uncorrected ratio is larger than even the maximum [O III]/Hβ ratio seen in the extreme outermost H II regions in Sc galaxies and in the "isolated extragalactic H II regions" (Searle and Sargent 1972) where the high excitation is due to very low heavy-element abundances.

We thus conclude that the H II regions in the outer parts of 3C 120 do not consist of gas of normal chemical composition being ionized by normal stars. The moderately strong [O II] λ3727 lines argue against the source of ionizing photons being a very hot blackbody, as is the case for planetary nebulae. The presence of strong forbidden lines of several different ionization species is characteristic of the narrow-line regions of quasars, Seyfert galaxies, and some radio galaxies (Baldwin 1975; Koski 1978; Osterbrock 1978), where the high excitation is caused by a strong nonthermal ultraviolet continuum. Table 3 lists the spectrum of an "average" type 2 Seyfert galaxy (from Koski 1978), and the agreement with the data for 3C 120 is quite good. As a further check, we have used a computer program made available to us by Dr. G. Shields (see Shields 1978) to generate models representing low-density gas clouds photoionized by a dilute power-law radiation field, which simulates the 3C 120 nucleus as seen from Region 2. Once again the agreement with the 3C 120 observations is quite good[3]. Since we already know that 3C 120 has a strong power-law continuum source in its center, we suggest (as have Balick and Heckman 1979) that this is likely to be the dominant excitation mechanism in the outer regions of 3C 120 as well as in the nucleus.

The Hα flux from Region 2 corresponds to $N_e N_{H^+} V = 10^{62}\ \mathrm{cm}^{-3}$ (where V is the volume in cm^3) and to a mass $M(H^+) = (10^5/N_e)M_\odot$. Our limit on the ([O III] λ4363)/([O III] λ5007) intensity ratio gives $N_e < 10^7\ \mathrm{cm}^{-3}$ in the O^{++} zone for any reasonable temperature ($T_e > 5000$ K). The presence of the density-sensitive [O II] λ3727 doublet shows that at least part of the gas has $N_e < 10^3\ \mathrm{cm}^{-3}$, which in turn gives a mass limit $M(H^+) > 100\ M_\odot$. The only lower limit on N_e comes from setting an upper limit on the volume occupied by the gas. The surface area of Region 2 can be no more than $1.6 \times 3.2\ \mathrm{kpc}^2$, and we consider it to be extremely unlikely that its depth along the line of sight exceeds 50 kpc, the projected diameter of 3C 120. An H II region uniformly filling this volume with $N_e \sim 5 \times 10^{-3}\ \mathrm{cm}^{-3}$ would produce the observed Hα flux. In all probability the gas is far thinner than 50 kpc and is also clumpy, but as we do not know the appropriate thickness or filling factor, we can only set an upper limit of $M(H^+) < 10^8\ M_\odot$.

A lower limit on the O/H abundance ratio in Region 2 can be derived from the estimated λ5007/Hβ intensity ratio. If the oxygen ionization zones are reasonably well defined,

$$\frac{N(\mathrm{O})}{N(\mathrm{H})} \geq \frac{N(\mathrm{O}^{++})}{N(\mathrm{H}^+)} \geq \frac{I(\lambda 5007)}{I(\mathrm{H}\beta)} f(T_e)\,,$$

where $f(T_e)$ is the ratio of the emission coefficients for the Hβ and [O III] lines and is an increasing function of the electron temperature T_e. The upper limit on the strength of the [O III] λ4363 line indicates that $T_e <$ 30,000 K. We have used Shield's computer program to run models of Region 2 in which the gas is photoionized by a variety of continuum shapes and for a wide range of heavy-element abundances (down to 10^{-5} of the solar value), and we found that the temperature in the O^{++} zone always lies in the range 9000–14,000 K. Taking 25,000 K as a very conservative upper limit for T_e, we find that $N(\mathrm{O})/N(\mathrm{H}) > 3 \times 10^{-5}$. This is within a factor of about 20 of the solar oxygen abundance. For a temperature of 10,000 K the O/H abundance ratio would be about equal to the solar value. These results are entirely consistent with the abundance normally found at this radial distance in the disks of spiral galaxies, but are clearly very much larger than extreme Population II abundances.

The other abundance-sensitive line ratio which we were able to measure in Region 2 is I([N II] λ6548 + λ6584)/I([O II] λ3727) ~ 2. This ratio is, again, fairly sensitive to the electron temperature, and our estimate of the Hα/Hβ intensity ratio suggests that a reddening correction of up to a factor of 2 may be needed, but for $5000 < T_e < 25{,}000$ K the N^+/O^+ abundance ratio agrees with the solar value to within a factor of 10.

The emission line spectrum of Region 1 is very similar to that of Region 2, although the spectra do not extend to Hα or the [N II] lines (see Table 3). The two regions also have about the same surface brightness in the λ5007 line, so the conclusions reached for Region 2 about the ionization mechanism and gas masses may also be applied to Region 1. Table 4 lists measurements or upper limits on the emission-line strengths in the other regions observed at low resolution, but the relative strengths of the λ5007 emission lines from the different regions are fairly uncertain because of the poor photometric conditions.

[3] This good agreement is something of a mixed blessing, however, because in a wide variety of situations this sort of model calculation is found to predict a λ3727/5007 intensity ratio, which is about an order of magnitude smaller than the observed values; see Shields (1978).

TABLE 4

EMISSION LINE STRENGTHS FOR REGIONS 1–13

Region	$\frac{I(3727)}{I(5007)}$	$\frac{I(H\beta)}{I(5007)}$	$\frac{I(H\alpha+N\,II)}{I(5007)}$	$F(5007)$ (10^{-15} ergs cm^{-2} s^{-1})	$W_\lambda(5007)$ (Å, obs. frame)
1.....	0.20	0.08	...	6	40
2.....	0.17	< 0.06	0.63	4	60
3.....	...	< 0.5	...	0.9:	20:
4.....	...	≤0.07	...	3	40
5.....	...	...	...	< 2	< 300
6.....	...	≤0.17	1.9	3	40
7.....	0.13	0.06:	...	5	100
8.....	...	< 0.3	...	6	50
9.....	...	< 0.3	1.2	8	11
10.....	...	...	...	< 2	< 800
11.....	...	...	...	4	70:
12.....	< 0.5	≤0.10	...	8	300:
13.....	...	...	...	1	20:

Returning to the discussion of the source of the ionizing photons, we note that the Hα flux from Region 2 corresponds to about 10^{49} ionizing photons s^{-1}. This is a very small fraction ($\sim 10^{-3}$) of the total number of ionizing photons which would be emitted by the 3C 120 nucleus if it has a power-law spectrum with $\alpha = 1$. Region 2, as seen from the nucleus, would have to subtend a solid angle of 0.01 steradians to intercept this number of photons. If the emission comes from a single cloud filling the whole 6.4 kpc projected length of the spectrograph slit, the cloud would need to be only 100 pc thick along the line of sight. None of these statements contradicts our hypothesis that Region 2 is ionized by the radiation from the nucleus.

Regions 1 and 2 have about the same relative line intensities and have λ5007/3727 intensity ratios which are about 6 times smaller than that of the nucleus. To see if this is consistent with the effects of a changing dilution factor, we have again used Shields's computer program to run a grid of models representing low-density, optically thick gas clouds at different distances from the 3C 120 nucleus. These models predict that the λ5007/Hβ intensity ratio should not drop by more than 25% until the distance from the nucleus is somewhat greater than 10 kpc, but that the λ5007/3727 ratio should drop rapidly out to 20 kpc (decreasing by a factor of 15 between 1 and 10 kpc) and then should level off. Given the uncertainty in the true distances from the nucleus of Regions 1 and 2 (because of the unknown projection factors), these observations are also consistent with the nucleus being the source of the ionizing photons. Future long-slit spectrophotometry over a wavelength range including the λ3727, Hβ, and λ5007 lines and covering a greater fraction of the surface area of 3C 120 will offer a better test.

III. VELOCITY MAP

a) Observations

The second phase of our investigation was to make a two-dimensional velocity map over the surface of the galaxy. These velocities were measured from the [O III] λ5007 emission line, the strongest emission line visible on the low-resolution data. Spectra were taken on the nights of 1977 Oct. 16, 17, and 18, using the Image Photon Counting System (IPCS) (Boksenberg 1972) on the Anglo-Australian telescope. A long spectrograph slit was used to obtain 13 spectra simultaneously, each covering 4″ along the slit by 2″ across the slit. The slit was aligned parallel to the major axis of 3C 120 as measured from Arp's plate (position angle 117°), and spectra were taken with the center of the slit at 11 different points along the corresponding minor axis to produce a systematic grid of 143 spectra.

The spectra cover the wavelength range 4827–5481 Å, which is centered on the redshifted position of the [O III] λ5007 emission line and also covers the [O III] λ4959 and Hβ lines, and the instrumental resolution is 1 Å (~ 60 km s^{-1}). We normally made 100 s exposures on the nebulosity, taking between one and four exposures at each position (see Table 5). No correction for the sky background was made because it does not affect the measured velocity or intensity of the λ5007 emission line. We took short exposures on a comparison lamp at least as often as after every third exposure on the nebulosity, and all of our

TABLE 5

HIGH-DISPERSION SPECTRA

Night	Δy Position of Slit	Integration Time (s)
1978 Oct. 16.....	0	3750 (through cirrus)
1978 Oct. 17.....	+4	4000
1978 Oct. 17.....	−4	4000
1978 Oct. 17.....	−16	1750
1978 Oct. 17.....	+10	500
1978 Oct. 17.....	0	725
1978 Oct. 18.....	0	400
1978 Oct. 18.....	−2	2000
1978 Oct. 18.....	−10	3000
1978 Oct. 18.....	+20	1000
1978 Oct. 18.....	+6	2000
1978 Oct. 18.....	+2	1000
1978 Oct. 18.....	−6	1000

TABLE 6

[O III] λ5007 VELOCITIES IN 3C 120

Δy (arcsec)	Δx (arcsec)	F(5007) (10^{-16} ergs cm^{-2} s^{-1})	V_{min}[a]	V_{max}[a]	V_{peak}[a]
+20.....	−24	9.0	−116	−50	−100
	−20	9.0	−50	0	−50
	−16	9.0	−50	+133	+17
	−12	19.0	+17	+66	+50
	−8	16.0	−17	+166	+66
	−4	18.0	0	+133	+17
	0	29.0	+17	+100	+83
	+4	16.0	+100	+166	+100
	+8	7.0	+182	+265	+232
+10.....	−12	14.0	+66	+199	+199
	−8	11.0	−100	+100	0
	−4	65.0	−50	+66	0
	0	47.0	−33	+100	+66
	+4	36.0	−33	+116	+66
	+8	15.0	+66	+149	+83
+6.....	−12	4.0	+166	+100	−50
	−8	10.0	−100	−50	−83
	−4	49.0	−66	+149	−50
	0	63.0	−50	+149	0, +116
	+4	29.0	0	+265	+116
	+8	9.0	−83	+498	+116
+4.....	−16	0.5	...	...	−66:
	−12	5.0	−216	−116	−133
	−8	14.0	−149	−66	−100
	−4	55.0	−116	+149	−50
	0	180.0	−33	+133	0, +100
	+4	58.0	+33	+182	+133
	+8	11.0	−17	+199	+66
+2.....	−12	10.0	−182	+149	−166
	−8	8.0	−182	−50	−116
	−4	95.0	−66	+33	−17
	0	620.0	−17	+66	+33
	+4	57.0	+83	+199	+133
	+12	4.0	...	...	+149:
0.....	−12	7.0	−216	+33	−166
	−8	32.0	−133	+199	−66
	−4	470.0	−166	+83	−17
	0	2100.0	−100	+66	0
	+4	290.0	−33	+133	+83
	+8	18.0	−182	+216	+66
−2.....	−8	13.0	−100	+232	−66
	−4	390.0	−149	+232	−100
	0	1300.0	−116	+50	−33
	+4	64.0	−182	+199	−133, +116
	+8	2.0	...	...	−116:
−4.....	−8	5.0	−199	−50	−116
	−4	130.0	−149	−66	−116
	0	270.0	−133	−33	−83
	+4	65.0	−199	+166	−17
	+8	8.0	−149	+149	+83:
−6.....	−8	4.0	...	...	−182:
	−4	26.0	−232	+199	+66
	0	22.0	−199	+50	−149, +17
	+4	6.0	−149	+33	−83
	+24	1.0	...	...	+166:
−10.....	−12	5.0	−614	−315	−464
	−8	21.0	−514	−249	−299
	−4	14.0	−464	−50	−182
	0	24.0	−464	−17	−83
	+4	2.0	−133	−50	−83
	+16	2.0	−83	+133	+33
	+20	3.0	+83	+100	+83
	+24	5.0	−50	+17	0
−16.....	−8	4.0	−531	−332	−398
	−4	10.0	−481	−265	−382
	0	17.0	−365	−50	−232
	+4	19.0	−149	−17	−83
	+8	17.0	−149	0	−50
	+12	11.0	−630	−83	−100
	+16	16.0	−116	−33	−116
	+20	18.0	−166	−83	−133
	+24	7.0	−265	−50	−166

[a] In km s^{-1}, relative to nucleus.

velocities for the λ5007 line have been measured relative to the positions of emission lines at 5162.28 and 5187.75 Å in the comparison arc spectrum taken closest in time to the particular spectrum of the nebulosity. Later analysis of the comparison arc spectra showed a maximum drift in the spectrograph's wavelength scale of 0.9 Å during the night and of about 0.4 Å hr^{-1}. By measuring the position of the λ5007 line relative to the positions of the nearest lines in arc spectra taken at nearly the same time, the effects of this wavelength drift are minimized, and we estimate the total internal error to be no more than ±0.6 Å. Measurements of the velocity of the nucleus made on three different nights and over a wide range of zenith distances agree to within ±0.4 Å and, thus, support this estimate of the uncertainties involved.

The grid of points used in the velocity map, superposed on Arp's plate of 3C 120, is shown in Figure 5. The corresponding velocities are listed in Table 6, relative to a radial velocity for the nucleus of 9920 km s^{-1}. The λ5007 line did not appear at every point observed, but we were able to measure velocities for the peak of the emission line at 72 points. In some cases there were two peaks of equal intensity, giving two velocities. Table 6 also lists the maximum and minimum velocity and an estimate of the integrated λ5007 intensity at each point. As can be seen in Figure 6, the λ5007 line is often many resolution elements wide, with a very irregular profile. We did not calibrate the spectra with observations of standard stars, so the intensities in Table 6 were determined by comparing the IPCS count rate for the λ5007 line from the nucleus to the flux for this line found from the low-resolution scans of the nucleus. The intensity scale is therefore subject to a large systematic uncertainty, possibly amounting to a factor of 2.

b) General Features of the Velocity Field

The first impression from Figures 5 and 6 and Table 6 is that the velocity field of the gas associated with 3C 120 is highly disordered. Even far from the nucleus there are discontinuities of over 100 km s^{-1} between the peak velocities in adjacent resolution elements, the emission lines coming from single 1.6 × 3.2 kpc resolution elements often have double peaks, and in extreme cases the profiles are as much as 400 km s^{-1} wide between the zero intensity points. But superposed on this chaos is a general pattern, discernible in Figure 5, of positive velocities in the northern half of 3C 120 (*upper right* in the figure) and negative velocities in the southern half. An approximate line of zero velocities falls in the vicinity of P.A. 72°. If the velocity structure is caused principally by rotation, this would be the minor axis of rotation. We have chosen P.A. 72° as the best-fitting direction for this axis by projecting major and minor axes onto the galaxy at a succession of position angles, and then finding the position angle that gave simultaneously the steepest velocity gradient along the major axis and the flattest along the minor axis. The uncertainty in this result is about ±15°.

TABLE 7

DERIVED MASS DISTRIBUTION OF 3C 120

R (kpc)	$V(R)$ (km s^{-1})	$M(R)$ (10^9 $M_\odot$)
2.....	130	0.4
6.....	130	1.0
10.....	240	6.0
14.....	590	60.0
18.....	180	7.0
22.....	310	20.0
26.....	160	8.0

The position angle of this axis, marked "rotation" in Figure 5, differs by 45° from the isophotal minor axis on Arp's plate. It is, however, quite close to the direction along which the compact radio source is expanding (P.A. 65°, marked "radio" in Fig. 5). Given the slight variability of the radio position angle (Cohen *et al.* 1977) and the uncertainty in the determination of the "rotation" axis, the two axes could easily coincide. There are other possible explanations besides rotation for the systematic trends in the velocity field of the gas: the expansion or contraction of a flattened structure is perhaps the most obvious, or a combined radial flow and rotation could skew the line of zero velocities from the true minor axis by an arbitrary amount.

In order to estimate the mass which would be required to produce circular velocities of the same order of magnitude as the velocities observed in 3C 120, we followed the techniques of Warner *et al.* (1973) to produce the crude rotation curve shown in Figure 7. This required the assumption that the gas is in generally circular motion about an axis at P.A. 72° and with an (arbitrarily chosen) 45° inclination to the line of sight. The assumption that the average velocities in different radial bins represent Keplerian motion about a point mass, then, gives the mass distribution listed in Table 7, where $M(R)$ is the total mass internal to each radial point. Although these mass estimates vary erratically at the larger radial distances, smoothing over the noise in the $M(R)$ curve suggests that, under the above assumptions, most of the mass would have to lie within a radius of 10 kpc and would be of the order 10^{10} $M_\odot$, with a $(\sin i)^{-2}$ dependence on the inclination angle of the galaxy.

c) Cloud Structure

The complicated, often double-peak structure superposed on the overall velocity pattern can be interpreted as due to the projection of several, very large clouds overlapping along the line of sight. The boundaries of these clouds are often not well defined—there are also smooth velocity gradients across the face of 3C 120—but they are approximately as shown in Figure 8. There are large patches of gas with positive velocity even to the left of our "rotation" axis, and gas with negative velocities can be found to the right. There are also large velocity discontinuities at the bottom of Figure 8, where there appears to be a

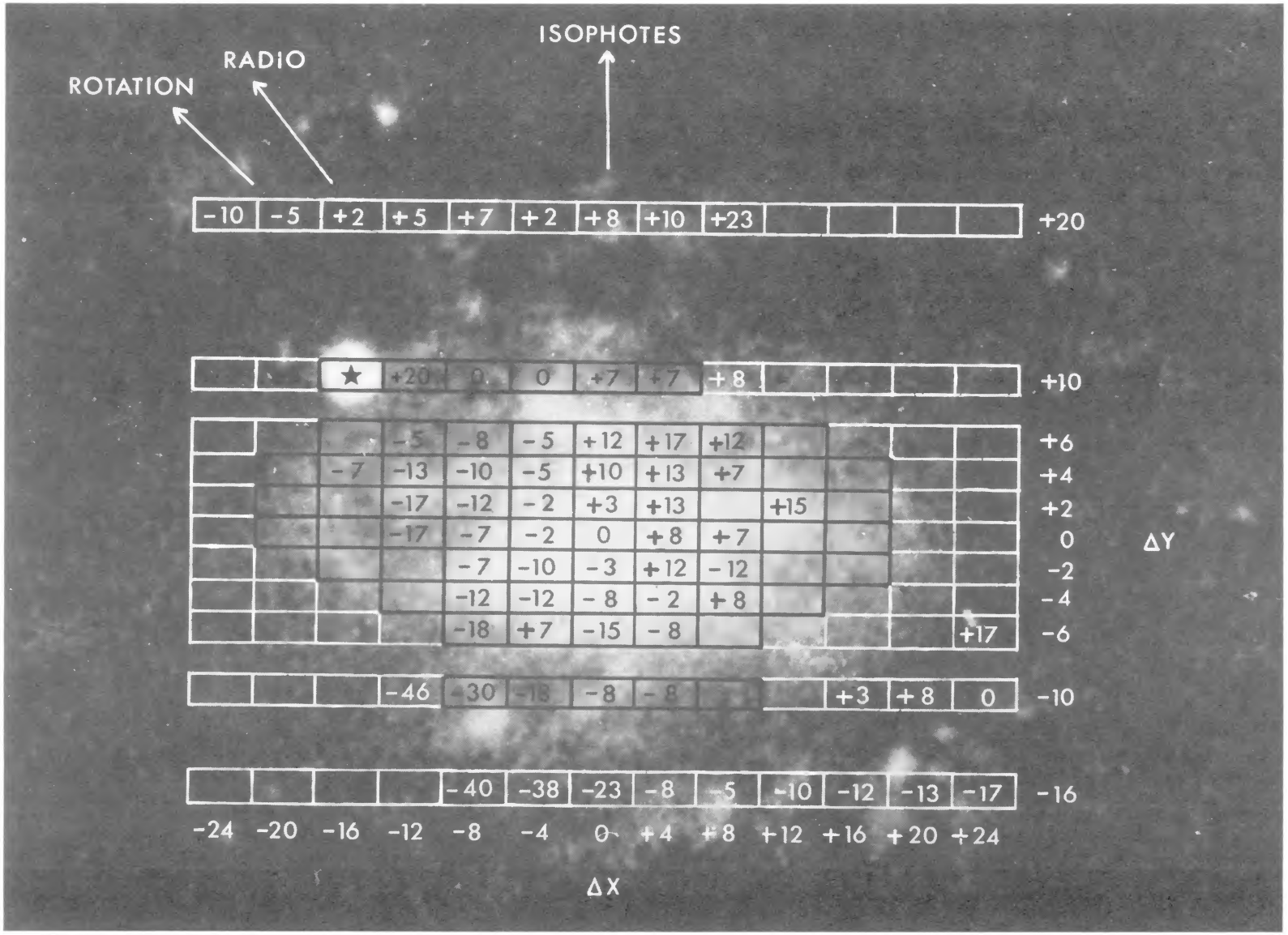

FIG. 5.—Direct plate of 3C 120 (from Arp 1975), with boxes showing regions observed at 1 Å resolution with IPCS. The numbers in the boxes represent velocities of the λ 5007 emission line at peak intensity (velocities are relative to the nucleus, and in units of 10 km s^{-1}). The Δx, Δy coordinate system is in arcsec from the nucleus, with the Δy axis at P.A. 27°.

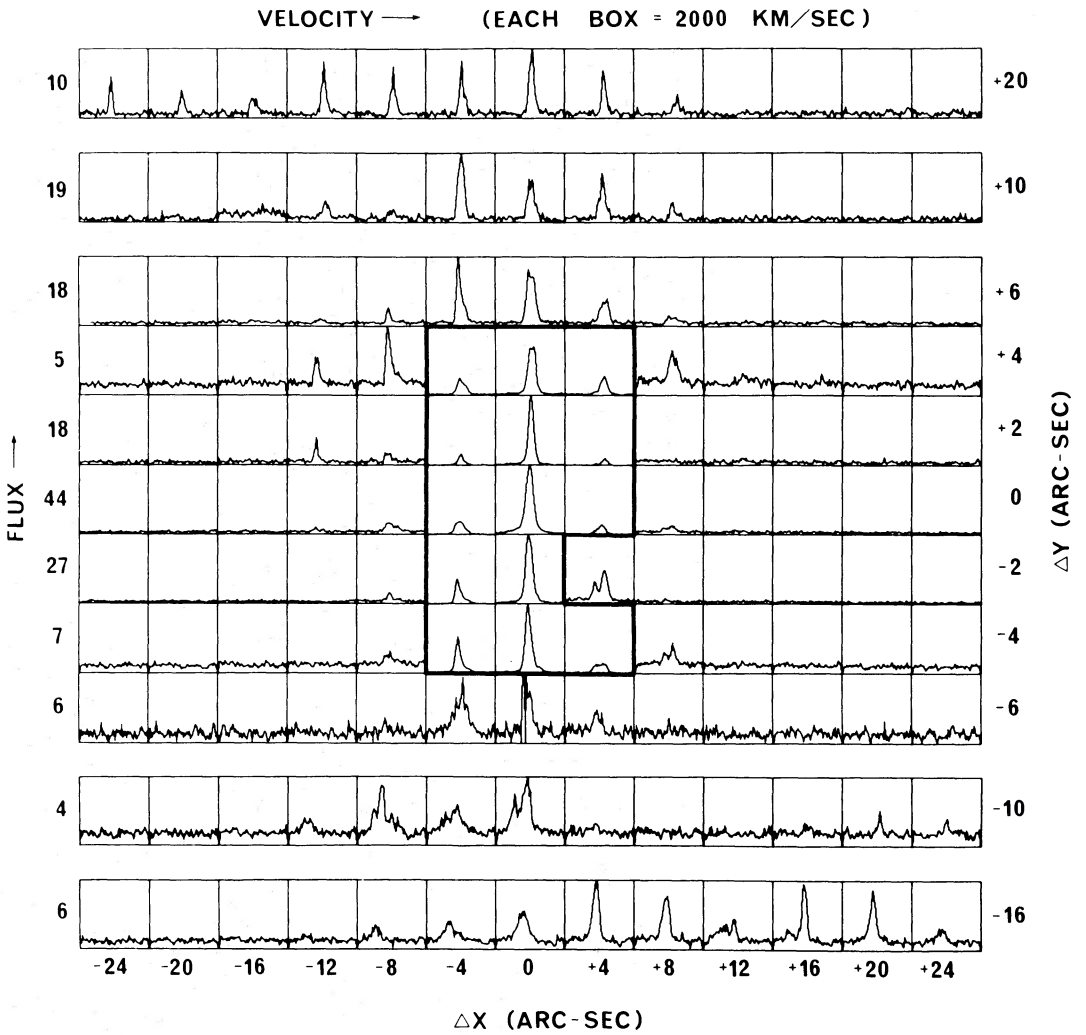

FIG. 6.—The λ5007 emission-line profiles at each Δx, Δy point shown in Fig. 5. The numbers along the flux axis are estimates, for each row, of the flux corresponding to the full height of the box (in units of 10^{-27} ergs cm^{-2} s^{-1} Hz^{-1}). The heights of the profiles have been reduced by a factor of 10 inside the area near the center which has been boxed off by heavy lines.

cloud moving toward us at 300–400 km s^{-1} (with respect to the nucleus) in the $\Delta x < 0$, $\Delta y < -4$ part of the galaxy, and then much more moderate velocities in the outermost filamentary structure at $\Delta x > 0$, $\Delta y = -16$. In view of the foregoing, it appears that even where the broad profiles cannot be separated into individual cloud components, the most plausible explanation of the broadening is that it is due to the superposition of several clouds along the line of sight, rather than to a very large velocity dispersion within a single cloud.

d) Surface Brightness Distribution

The isophotes of the λ5007 emission appear to have a significantly different shape from those of the underlying stellar population. This can be seen in Figure 5, where the direct plate taken by Arp has a passband extending from 3900 to 5400 Å and thus includes a long stretch of the underlying continuum as well as the redshifted λ5007 line. The λ5007 emission comes from the brightest areas on Arp's plate, but does not follow the outline of the fainter structure, which is elongated in the Δx direction. These underlying features can be seen clearly in the direct electronographic material published by Lelièvre (1976), where they are designated "Region 3." The λ5007 isophotes in the main part of the galaxy are approximately circular, but could be somewhat elongated in the Δy direction, perpendicular to the underlying, presumably stellar continuum. The outer filamentary structure and its accompanying λ5007 emission is skewed around in still another direction; in fact, the position angle along which the compact radio source is expanding has the largest projected dimensions of any of the optical structure in 3C 120.

Summing the total λ5007 flux from all of the points

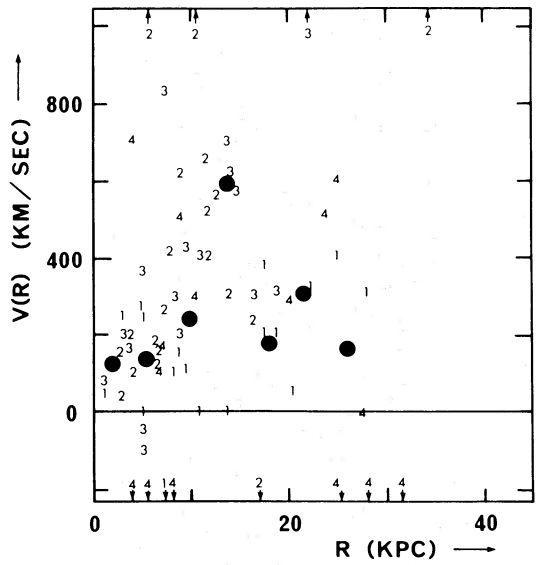

FIG. 7.—Rotation curve for 3C 120, arbitrarily assuming that the observed radial velocities represent the projected circular velocities of a disk of gas with minor axis at P.A. 72° and inclination 45°. The plotted symbols 1–4 represent the quadrant of the galaxy containing each point, measured around to the west from P.A. 72°. The large filled circles are weighted averages of the points in each radial bin.

observed at high dispersion, we find $F(\lambda 5007)_{\rm total} \sim 7 \times 10^{-13}$ ergs cm^{-2} s^{-1}. This is about 200 times the flux observed from Region 2, so the total mass estimate for all of the gas would scale up to $1 < M(H^+) < 10^{10}\ M_\odot$. If most of the gas is at low enough density to produce [O II] λ3727 emission, the lower limit can be raised to $10^4\ M_\odot$, while if the gas is in a moderately thin disk, the upper limit drops to about $10^8\ M_\odot$. Over half of the total λ5007 flux comes from within 3″ of the nucleus.

If our hypothesis (from § II) is correct in that the gas is photoionized by the nucleus, and if the volume filling factor is independent of radial distance from the nucleus in a disklike distribution, we would expect the surface brightness in the λ5007 line to fall off roughly as r^{-2} because of the changing dilution factor. From the data in Table 6, we find this to be the case for the main body of the galaxy, out to a radius of about 10 kpc. Farther out the surface brightness stays about constant in the spots where any emission is visible at all, but, as we concentrated in the outer parts on Δy positions which would contain the most bright emission knots, we believe that the average filling factor has probably been artificially increased by our observing procedure.

IV. DISCUSSION

The data lead directly to several conclusions. First, the nebulosity surrounding the nucleus of 3C 120 contains stars having essentially the same redshift as the nucleus. Although we have only been able to show that the stars are present in Region 1, the continuum radiation in the other regions is consistent with a mixture of starlight plus the normal amount of

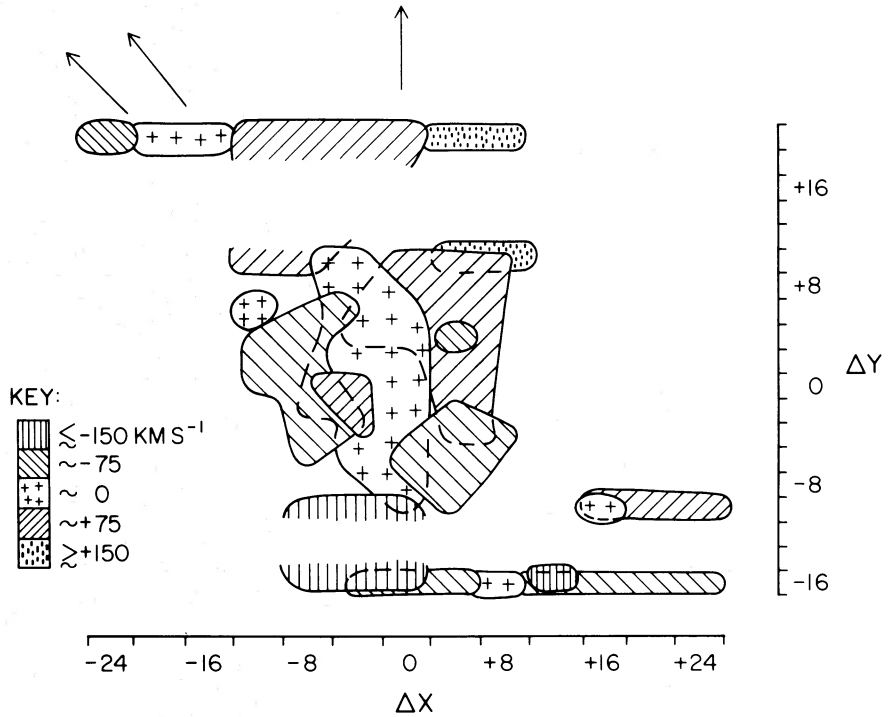

FIG. 8.—Schematic representation of the velocity structure in the λ5007 emission line, with the Δx, Δy coordinate system the same as in Figs. 5 and 6.

bound-free and free-free radiation from the H II regions. We cannot rule out other components, but any contribution from scattering of the light from the nucleus must be small because of the absence of broad Hβ emission.

Second, the H II regions are almost certainly photoionized, most probably by the strong nonthermal source in the nucleus. The relative intensities of the emission lines in the regions away from the nucleus, the gradient in relative intensities from the nuclear region to the outer parts, and the falloff in the surface brightness in the λ5007 line away from the nucleus all support the hypothesis that the nucleus is the source of the ionizing photons. The O/H abundance ratio in the nebulosity cannot be more than a factor of about 20 smaller than the solar value, while the N/O abundance ratio appears to be within a factor of 10 of the solar value.

Next, the velocity field of the ionized gas outside the nucleus is extremely disordered, with velocity spreads of up to 400 km s^{-1} in some of the 1.6 × 3.2 kpc^2 resolution elements, but an apparent rotation axis is still present at a position angle near 72°. This is roughly aligned with the axis along which the compact radio source in the nucleus is expanding (P.A. 65°). Both of these axes are rotated 45° from the minor axis of the outer optical isophotes (P.A. 27°).

Finally, the total mass of ionized gas outside the nucleus could lie anywhere in the range $1 < M(H^+) < 10^{10}\ M_\odot$, although 10^4–10^8 is a more likely range of values. The upper limit on the mass of neutral hydrogen is $M(H^\circ) < 2 \times 10^{10}\ M_\odot$ (Heckman, Balick, and Sullivan 1978).

We find it suggestive that the emission lines in the nebulosity surrounding 3C 120 have similar intensity ratios to the emission lines in the nebulosities associated with the QSOs 3C 48 (Wampler *et al.* 1975), 3C 249.1 (Richstone and Oke 1977), and 4C 37.43 (Stockton 1976). These results are listed in Table 3 for comparison with the 3C 120 values. In addition, both 3C 48 and 4C 37.43 show velocity differences (nebulosity–nucleus) of the order of 400 km s^{-1}, which is similar to our results for 3C 120. It is thus likely that our study of 3C 120 is relevant to these objects, in particular, and perhaps to the QSO phenomenon, in general.

We consider three possible models of the interaction between the observed ionized gas and the rest of the 3C 120 galaxy: (1) The gas may be the interstellar medium of a fairly normal galaxy which is being excited by the radiation field of the active nucleus. (2) The gas in the galaxy is in the process of being dynamically disrupted by the active nucleus, and much of the observed motion represents outflow. (3) The gas motions represent accretion of gas, unrelated to the galaxy itself, which is possibly fueling the violent activities in the nucleus.

1. *Is the gas simply the interstellar medium of a normal galaxy?* In this case, the gas already would have had essentially its present spatial distribution before the radiation field (or possibly the particle field) of the nucleus started to act on it. Our present upper limit on the total gas mass does not rule out a spiral galaxy; we might expect as much as $10^{10}\ M_\odot$ of gas for a large late-type spiral. On the other hand, our lower limit for the gas mass is easily consistent with an elliptical galaxy in which normally invisible gas is being excited by the nucleus. Further observations at Arecibo might be able to push the H I limit as low as $\sim 10^9\ M_\odot$ and, thus, offer some hope for a detection if 3C 120 is indeed a late-type spiral.

The very disordered velocity structure would presumably be due to momentum input from either the ionizing photons or a particle flow. We estimate that the gas outside the nucleus is presently absorbing momentum from the ionizing photons at a rate which would impart average velocities of 100 km s^{-1} in a time $10^8/N_e$ yr, so there is no difficulty in producing the observed disruptive velocities in a short time. Indeed, if the gas is in a disk and if we can rely on our crude rotation curve, the phenomenon *must* be short-lived because much of the gas is moving faster than the escape velocity, $2^{1/2}V_{\rm circular}$, and has a time scale for escape of less than $\sim 10^8$ yr.

These short time scales argue against the gas being in a relatively undisturbed state, as do the results that (*a*) the ionized gas has a different spatial distribution from that of the underlying galaxy, and (*b*) there is a misalignment between the "rotation" axis derived from the gas motions and the minor axis determined from the underlying elliptical structure. These factors lead us to believe that the spatial distribution of the gas in 3C 120 is too disturbed to tell us much about the normal state of the underlying galaxy.

2. *Is the gas systematically flowing away from the nucleus of 3C 120?* The line of zero velocities which we have been calling the "rotation" axis could be produced strictly by the geometrical arrangement of the outward-flowing gas. For instance, the "cloud" structure sketched in Figure 8 may be interpreted as large sheets of material expanding outward in two cones. The axis of this expansion would then be projected at a right angle to the line of zero velocities. If the expansion of the gas were being channeled perpendicular to the disk of a flattened galaxy, the major axis of the galaxy should be projected parallel to the line of zero velocities, rather than at a 45° angle as is observed. The axis of the radio expansion might also be expected to lie in approximately the same direction as that in which the ionized gas is expanding, instead of at the observed 90° angle. It is worth mentioning that many of the models of "superluminally" expanding radio sources require the source to be expanding along an axis pointed almost directly at us (Marscher and Scott 1980). Thus, small deviations between the three-dimensional orientations of various axes could appear as very large projected differences in position angle.

Alternatively, the systematic motion of the gas could be a combination of rotation and outflow. If the outflow velocity equaled the rotation velocity, the apparent minor axis of rotation would be skewed around by about 45° (not allowing for the inclination of the galaxy). This could explain the difference

between the position angles of our "rotation" axis and the "isophotal" minor axis from Arp's plate, but it would again imply that the approximate agreement between the "rotation" and radio-expansion axes is only a chance alignment. The observed velocity field is so disordered that we have not tried to fit it to a detailed model of this type.

Although the above picture is not entirely satisfactory, the idea of outward-expanding sheets of gas may still be correct. In either of the above situations the outward velocity, not allowing for projection effects, must be on the order of 100 km s^{-1} at 10 kpc. This is the escape velocity from a central mass of $2 \times 10^{11} M_{\odot}$. Thus, while some of the gas is likely to be unbound, it is not clear that all of it will be. The total kinetic energy of the outflow will be of order $10^{54}/N_e$ ergs. The radiation field from the nucleus could easily supply the required amounts of energy and momentum on relatively short time scales. It is also possible that the gas is being driven out of 3C 120 by some means other than radiation pressure. We note that the general structure of several discrete clouds moving in different directions with velocities of the order of the escape velocity is very similar to the situation inferred for the nuclei of other Seyfert galaxies (Walker 1968*a*, *b*; Ulrich 1972), except that the motions in 3C 120 have been observed over a much larger fraction of the galaxy. The velocity field in 3C 120 can also be compared to that found in the central region of the radio galaxy NGC 253, which appears to have ejected an expanding cone of gas along an axis inclined at somewhat less than 90° to the equatorial plane (Ulrich 1978).

3. *Is 3C 120 accreting a large gas cloud?* A third alternative is that 3C 120 is encountering a previously unrelated gas cloud, which, following a hypothesis put forward by Gunn (1979), is slowly feeding H I into the nucleus and thus providing fuel for its activity. If the line of zero velocities in Figure 5 is identified with a minor axis of rotation of the ionized gas, the difference between its position angle and that of the isophotal minor axis of the smooth luminosity distribution—which we presume to be due to stars and to represent the principal mass distribution—implies a system with two different axes of rotation.

Gunn (1979) suggested that the elliptical galaxy NGC 4278, which has a small-diameter, variable radio source in its nucleus, is accreting an intergalactic H I gas cloud of mass several times $10^8 M_{\odot}$. Knapp, Kerr, and Williams (1978) had shown from 21 cm observations that this gas appears to be rotating about an axis inclined at 70° to the minor axis of the stellar component of NGC 4278. Gunn discussed the dynamical interaction between such systems and pointed out that a strongly differential precession of a gas disk about the axis of symmetry of the stellar component would occur and would disrupt the gas disk.

There are several other possible examples of galaxies having two components with apparently unrelated dynamical properties. These include NGC 1052 (as discussed by Gunn 1979 and Fosbury *et al.*), the Seyfert galaxy NGC 1275, M82, the peculiar S0 galaxy NGC 2685, and the "ring galaxies," as well as the previously mentioned NGC 253. If one wishes to explain the phenomena in these objects and in particular in 3C 120 as being due to accretion of a massive H I intergalactic cloud, it is necessary to consider the number density of such clouds in space. Lo and Sargent (1979) searched 300 square degrees in three nearby groups of galaxies and found no discrete H I clouds. This led to upper limits on their spatial frequency of 0.15 Mpc^{-3} for clouds of mass greater than $8 \times 10^7 M_{\odot}$ and 0.02 Mpc^{-3} for clouds of mass greater than $\sim 4.6 \times 10^8 M_{\odot}$. Similarly, Haynes and Roberts (1979) found that there are no intergalactic H I clouds of mass greater than or equal to $10^8 M_{\odot}$ and galactic dimensions in the region of the Sculptor group of galaxies. Haynes and Roberts concluded that the clouds in this area of the sky, found by Mathewson, Cleary, and Murray (1975), are probably components of the Magellanic Stream. Finally the work of Lo and Sargent has led them to the conclusions that the Magellanic Stream itself is most probably not primordial gas but is the result of the interaction between the Magellanic Clouds and the Galaxy, that ring galaxies are not caused by collisions between spiral galaxies and intergalactic clouds, and that the accretion rate of H I onto normal isolated galaxies is negligible.

If we estimate that perhaps 1% of galaxies show "kinematic irregularities" similar to those in 3C 120 (a very uncertain estimate) and that the number of clouds is less than ~ 0.1 Mpc^{-3}, we can estimate the size of intergalactic H I clouds that would be needed to produce a collision in a Hubble time. We have

$$t \sim \frac{0.01}{n\sigma v} = H_0^{-1} .$$

For $H_0 = 50$ km s^{-1} Mpc^{-1}, $n = 0.1$ Mpc^{-3}, $v = 100$ km s^{-1}, we find $\sigma = 0.05$ Mpc^2, or a radius of about 100 kpc and a mass of $(10^{14} N_e) M_{\odot}$. It is thus possible to have large, tenuous intergalactic clouds of galactic mass or less (and which would be undetectable at the column density units set by Lo and Sargent or by Haynes and Roberts), but there is at present no positive evidence for their existence.

A second question regarding the accretion hypothesis comes from the observed heavy-element abundances, which appear to be nearly solar. Is it likely that these systems are accreting gas with solar metal abundances? There are several X-ray observations of Fe emission lines from large galaxy clusters (cf. Mitchell *et al.* 1976; Fabricant *et al.* 1980), but this emission may come from the immediate vicinity of one or a few galaxies rather than from the general intergalactic medium in the cluster. Also, 3C 120 is not in a cluster, nor is it associated with any other large galaxies. There is definitive evidence of the existence of enriched gas at least 16 kpc (and possibly as far as 60 kpc) from the center of the galaxy NGC 3067 (Boksenberg and Sargent 1978), as well as far out in the tails of some interacting galaxies (Schweizer 1978), but this is gas which has presumably evolved

as part of the parent galaxy rather than being representative of the sort of intergalactic material which might be encountered by a galaxy as isolated as 3C 120. Although we cannot rule out the possibility that 3C 120 is accreting previously unrelated gas having nearly solar metal abundances (it might, for instance be in the final stages of digesting another galaxy), we consider it more probable that the gas has been metal-enriched as part of a long history in association with 3C 120.

We conclude that the hypothesis that 3C 120 is accreting a large gas cloud, while attractive as an explanation of the peculiar velocity field in the hot gas in the disk of 3C 120 and for fueling the violent activity in the nucleus, can only be made plausible if it can be shown that there are sufficient metal-enriched intergalactic clouds in space, and present evidence is against this.

V. CONCLUSIONS

We have found that the nebulosity surrounding the nucleus of 3C 120 contains a stellar population having the same redshift as the nuclear emission-line region. This nebulosity also contains numerous H II regions which appear to be photoionized by the nucleus and which have heavy-element abundances that approach solar values.

The velocity structure of these clouds is so disorderly that they are unlikely to be in a dynamically stable configuration, and the general orientation of the emitting gas seems to be different from that of the underlying stellar population, so we conclude that the gas is being either expelled or accreted. Our velocity map shows an overall pattern in which the gas velocities, relative to the nucleus, are mostly positive to one side of an axis passing through the nucleus at P.A. 72° and mostly negative on the opposite side. This apparent axis is rotated some 45° from the minor axis of the faint, underlying elliptical structure (visible on previously published broad-band direct plates) which we presume to consist mainly of stars.

The observations are consistent with a general outflow of material, quite possibly of large sheets or clouds in a configuration resembling two opposed cones. But if we choose to equate the line of zeros in the velocity field of the gas with a minor axis of rotation, and if we assume that the underlying elliptical structure is an inclined disk of stars, then the difference between the rotation axes of the stellar and gas components is analogous to that recently found in the radio galaxy NGC 4278, and possibly also NGC 1052. This suggests the interpretation that 3C 120 is accreting a previously unrelated gas cloud. The high metal abundances found in the outlying H II regions and the observational limits on the frequency of such clouds argue against this interpretation, but do not completely rule it out. Our conclusion must be that although the gas presently associated with 3C 120 appears to be in wholesale motion, we cannot be sure from observational grounds alone whether the nucleus represents the source or the sink of these gas flows.

We have been able to get such a detailed look at 3C 120 partly because it is close, but probably also because the powerful continuum source in the nucleus has illuminated gas in the outlying regions which would otherwise be invisible optically. We hope that a systematic survey of other fairly luminous but nearby objects like 3C 120 can yield further candidates for detailed study, so that we can eventually find the properties which these quasar-like galaxies have in common and their relation to QSOs themselves.

We wish to acknowledge the use of H. C. Arp's beautiful photograph of 3C 120 for our illustrations. This work has benefited from enlightening conversations with numerous colleagues, among whom we would particularly like to thank M. Begelman, M. Phillips, R. Sanchissi, F. Schweizer, and A. M. Wolfe. We are grateful to the staffs of the Anglo-Australian, Cerro Tololo, Lick, and Kitt Peak Observatories for assisting us in obtaining the observations, and to C. Mackay for access to the Nova computer on which much of the data reduction was done. We wish to thank E. O. Smith for her work on the photographic illustrations.

J. A. B., A. B., and R. F. C. acknowledge support from the UK Science Research Council, and J. A. B. and E. J. W. from the National Science Foundation. At UCSD, research in extragalactic astronomy is supported in part by NASA under grant NSG 7377 and in part by the National Science Foundation under grant AST 77-22560.

REFERENCES

Adams, T. F., and Weedman, D. W. 1975, *Ap. J.*, **199**, 19.
Arp, H. 1975, *Pub. A.S.P.* **87**, 545.
Atwood, B., Ingerson, T., Lasker, B. M., and Osmer, P. S. 1979, *Pub. A.S.P.*, **91**, 120.
Baldwin, J. A. 1975, *Ap. J.*, **201**, 26.
Baldwin, J. A., Rees, M. J., Longair, M. S., and Perryman, M. A. C. 1978, *Ap. J. (Letters)*, **226**, L57.
Balick, B., and Heckman, T. 1979, *A.J.*, **84**, 302.
Boksenberg, A. 1972, *Proc. ESO/CERN Conf. on Auxiliary Instrumentation for Large Telescopes*, ed. S. Laustsen and A. Reiz (Geneva: ESO—Telescope Division), p. 295.
Boksenberg, A., and Sargent, W. L. W. 1978, *Ap. J.*, **220**, 42.
Bowen, I. 1934, *Pub. A.S.P.*, **46**, 146.
Brocklehurst, M. 1971, *M.N.R.A.S.*, **153**, 471.
Burbidge, E. M. 1967, *Ap. J. (Letters)*, **149**, L51.
Canfield, R. C., and Puetter, R. C. 1980, *Ap. J. (Letters)*, in press.
Cohen, M. H. *et al.* 1977, *Nature*, **268**, 405.
Dopita, M. A. 1977, *Ap. J. Suppl.*, **33**, 437.
Fabricant, D., Topka, K., Harnden, F. R., and Gorenstein, P. 1980, preprint.
Feldman, F. R., and MacAlpine, G. M. 1978, *Ap. J.*, **221**, 486.
Ferland, G., and Netzer, H. 1979, *Ap. J.*, **229**, 274.
Fosbury, R. A. E., Mebold, U., Goss, W. M., and Dopita, M. A. 1978, *M.N.R.A.S.*, **183**, 549.
Gunn, J. E. 1979, in *Active Galactic Nuclei*, ed. C. Hazard and S. Mitton (Cambridge: Cambridge University Press), p. 213.
Haynes, M., and Roberts, M. 1979, *Ap. J.*, **227**, 767.
Heckman, T. M., Balick, B., and Sullivan, W. T., III. 1978, *Ap. J.*, **224**, 745.

Knapp, G. R., Kerr, F. D., and Williams, B. 1978, *Ap. J.*, **222**, 800.
Koski, A. T. 1978, *Ap. J.*, **223**, 56.
Krolik, J., and McKee, C. 1978, *Ap. J. Suppl.*, **37**, 459.
Lelièvre, G. 1976, *Astr. Ap.*, **51**, 347.
Lo, K. Y., and Sargent, W. L. W. 1979, *Ap. J.*, **227**, 756.
MacAlpine, G. M. 1976, *Ap. J.*, **204**, 694.
Marscher, A. P., and Scott, J. S. 1980, *Pub. A.S.P.*, in press.
Mathewson, D. S., Cleary, M. N., and Murray, J. D. 1975, *Ap. J. (Letters)*, **195**, L97.
Miller, J. S., Robinson, L. B., and Wampler, E. J. 1975, *Adv. Electron. Electron Phys.*, **40**, 693.
Mitchell, R. J., Culhane, J. J., Davison, P. J. N., and Ives, J. C. 1976, *M.N.R.A.S.*, **176**, 29.
Oke, J. B. 1974, *Ap. J. Suppl.*, **27**, 21.
Osterbrock, D. E. 1978, *Phys. Scripta*, **17**, 137.
Peimbert, M., and Costero, R. 1969, *Bol. Obs. Tonantzintla y Tacubaya*, **5**, 3.
Phillips, M. M., and Osterbrock, D. E. 1975, *Pub. A.S.P.*, **87**, 949.
Puetter, R. C., Smith, H. E., and Willner, S. P. 1979, *Ap. J. (Letters)*, **227**, L5.
Puetter, R. C., Smith, H. E., Soifer, B. T., Willner, S. P., and Pipher, J. L. 1978, *Ap. J. (Letters)*, **226**, L53.
Richstone, D. O., and Oke, J. B. 1977, *Ap. J.*, **213**, 8.
Rieke, G. H., and Low, F. J. 1972, *Ap. J. (Letters)*, **176**, L95.
Schnopper, H. W., Epstein, A., Delvaille, J. P., Tucker, W., Doxsey, R., and Jernigan, G. 1977, *Ap. J. (Letters)*, **215**, L7.
Schweizer, F. 1978, in *Structure and Properties of Nearby Galaxies*, eds. E. Berkhuijsen and R. Wielebinski (Dordrecht: Reidel), p. 279.
Searle, L. 1971, *Ap. J.*, **168**, 327.
Searle, L., and Sargent, W. L. W. 1972, *Ap. J.*, **173**, 25.
Seaton, M. J. 1960, *Rept. Progr. Phys.*, **23**, 313.
Shields, G. A. 1974, *Ap. J.*, **191**, 309.
———. 1978, *Ap. J.*, **219**, 565.
Shields, G. A., Oke, J. B., and Sargent, W. L. W. 1972, *Ap. J.*, **176**, 75.
Smith, H. E. 1975, *Ap. J.*, **199**, 591.
Soifer, B. T., Oke, J. B., Mathews, K., and Neugebauer, G. 1979, *Ap. J. (Letters)*, **227**, L1.
Stockton, A. 1976, *Ap. J. (Letters)*, **205**, L113.
Stone, R. P. S. 1977, *Ap. J.*, **218**, 767.
Ulrich, M.-H. 1972, *Ap. J. (Letters)*, **171**, L37.
———. 1978, *Ap. J.*, **219**, 424.
Walker, M. 1968*a*, *A.J.*, **73**, 854.
———. 1968*b*, *Ap. J.*, **151**, 71.
Walker, M. F., Pike, C. D., and McGee, J. D. 1974, *Pub. A.S.P.*, **86**, 870.
Wampler, E. J. 1968, *A.J.*, **73**, 855.
Wampler, E. J., Robinson, L. B., Burbidge, E. M., and Baldwin, J. A. 1975, *Ap. J. (Letters)*, **198**, L49.
Warner, P. J., Wright, M. C. H., and Baldwin, J. E. 1973, *M.N.R.A.S.*, **163**, 163.
Weedman, D. W. 1976, *Ap. J.*, **208**, 30.
Wlérick, G., Westerlund, B., and Garnier, R. 1979, *Astr. Ap.*, **72**, 277.

J. A. BALDWIN: Cerro Tololo Inter-American Observatory, Casilla 63-D, La Serena, Chile

A. BOKSENBERG: Department of Physics and Astronomy, University College, Gower Street, London, England

E. M. BURBIDGE and H. E. SMITH: Department of Physics, University of California at San Diego, C-011, La Jolla, CA 92093

R. F. CARSWELL: Institute of Astronomy, Madingley Road, Cambridge CB3 0HA, England

E. J. WAMPLER: Lick Observatory, University of California at Santa Cruz, Santa Cruz, CA 95064